

**FABRICATION AND CHARACTERIZATION OF
GRAPHENE-BASED INK**

MOHD SAIDINA BIN DANDAN SATIA

**UNIVERSITI SAINS MALAYSIA
2019**

FABRICATION AND CHARACTERIZATION OF GRAPHENE-BASED INK

by

MOHD SAIDINA BIN DANDAN SATIA

**Thesis submitted in fulfilment of the requirements
for the degree of
Doctor of Philosophy**

October 2019

ACKNOWLEDGEMENT

بِسْمِ اللَّهِ الرَّحْمَنِ الرَّحِيمِ

In the name of Allah, the Most Beneficent and the Most Merciful. All praises and thanks be to Allah for the strength, knowledge, ability and opportunity to undertake this research study and complete it satisfactorily. His blessings have made this achievement possible. Alhamdulillah.

First, deepest appreciation to my main supervisors in Universiti Sains Malaysia (USM), Malaysia and Université de Lorraine, France; Prof. Ir. Dr. Mariatti Jaafar and Prof. Claire Hérold for their guidance and supervision throughout this research. Their constant support, encouragement and credible ideas have been great inspirations in the completion of the thesis. Also to my co-supervisors; Dr. Syazana Ahmad Zubir and Dr. Sébastien Fontana, for their helpfulness and continuous support in the completion of the research.

Acknowledgements are also extended to the School of Materials and Mineral Resources Engineering, Universiti Sains Malaysia and Institut Jean Lamour, Université de Lorraine for the great facilities and working space. Also, warmest appreciation to the SMMRE's and IJL's staffs for the administrative and technical supports provided.

Special thanks to the Ministry of Higher Education Malaysia (MyBrain15), Fundamental Research Grant Scheme (FRGS; Grant No. 6071385) and Campus France for granting the research fund used for this project.

To my dear friends Shahrul Affendi, Alif Nur Faizal, Andre Ningkan, Nurliyana, Naqib, Badrul, Dr. Nawal, Dr. Brigitte, Yoni Levy, Lilian, Anna, Hugo, Xavier, Tristan, Olivier, Illies and Syafiq, who always be there for me and kept me going on my path to success in whatever manner possible. Thanks for the friendship and memories.

Lastly, to the biggest source of my strength; my father and my late mother Hj. Dandan Satia Bin Bukah & Allahyarhamah Saimah Binti Pidu, my beloved sisters Samee'ah and Syawal, my brother, Saidani and his wife, Hafizatunisa and their children Hiliy and Hilfiy. Thank you for your tremendous love and constant encouragement that helped me through the difficult moments of reaching my dreams. Not forgetting my lovely cousins Ain, Kamisah, Khadijah, Syikin and Syafiqah, my adopted family Jasmi and Saliza, and their daughters Izni, Izzati, Ika, Munirah and Ida, my aunts and uncles, for their love and care. To those contributed in this research one way or another, your kindness means a lot to me. Thank you!

I would like to dedicate this work to my father and my late mother. This one is for both of you!

TABLE OF CONTENTS

| | |
|---|--------------|
| ACKNOWLEDGEMENT..... | ii |
| TABLE OF CONTENTS..... | iv |
| LIST OF TABLES | viii |
| LIST OF FIGURES | xi |
| LIST OF SYMBOLS..... | xvii |
| LIST OF ABBREVIATIONS..... | xix |
| ABSTRAK | xxi |
| ABSTRACT | xxiii |
| RÉSUMÉ..... | xxiv |
| CHAPTER 1 INTRODUCTION..... | 1 |
| 1.1 Background | 1 |
| 1.2 Problem statements..... | 4 |
| 1.3 Objectives | 7 |
| 1.4 Scope of study | 8 |
| 1.5 Thesis overview..... | 8 |
| CHAPTER 2 LITERATURE REVIEW | 10 |
| 2.1 Conductive ink materials..... | 10 |
| 2.1.1 Graphene-based ink | 13 |
| 2.1.2 Other conductive materials-based ink | 21 |
| 2.1.2(a) Ink based on conductive nanomaterials..... | 21 |
| 2.1.2(b) Ink based on conductive polymers | 22 |
| 2.1.3 Graphene hybrid-based ink..... | 24 |
| 2.2 Conductive ink properties | 26 |
| 2.2.1 Viscosity | 27 |
| 2.2.2 Surface tension | 28 |

| | | |
|---|--|-----------|
| 2.2.3 | Solubility parameters | 33 |
| 2.3 | Conductive ink stability..... | 34 |
| 2.3.1 | Ultraviolet-visible spectrophotometer | 34 |
| 2.3.2 | Zeta potential analysis | 36 |
| 2.4 | Flexible electronics..... | 38 |
| 2.4.1 | Methods to fabricate flexible electronics..... | 39 |
| 2.4.1(a) | Screen printing..... | 40 |
| 2.4.1(b) | Spray coating | 41 |
| 2.4.1(c) | Inkjet printing | 43 |
| 2.4.2 | Flexible electronics for the strain sensor | 45 |
| 2.5 | Summary | 50 |
| CHAPTER 3 MATERIALS AND METHOD | | 52 |
| 3.1 | Materials..... | 52 |
| 3.1.1 | Raw materials | 53 |
| 3.1.1(a) | Graphene-based materials..... | 53 |
| 3.1.1(b) | Silver nanoparticles | 53 |
| 3.1.1(c) | Poly(3,4-ethylenedioxythiophene)-poly(styrenesulfonate)..... | 54 |
| 3.1.2 | Solvents and chemicals..... | 55 |
| 3.2 | Experimental methods..... | 57 |
| 3.2.1 | Synthesis of graphene foam..... | 57 |
| 3.2.2 | Production of graphene-based ink for spray coating | 60 |
| 3.2.2(a) | Preparation of ink | 60 |
| 3.2.2(b) | Fabrication of conductive ink pattern | 60 |
| 3.2.3 | Production of graphene-based ink for inkjet printing..... | 62 |
| 3.2.3(a) | Different types of solvents..... | 62 |
| 3.2.3(b) | Mixed solvents..... | 62 |
| 3.2.3(c) | Fabrication of conductive ink pattern | 63 |

| | | |
|---|---|-----------|
| 3.3 | Characterization techniques | 65 |
| 3.3.1 | Scanning electron microscopy | 65 |
| 3.3.2 | High resolution transmission electron microscopy | 65 |
| 3.3.3 | X-ray diffraction | 66 |
| 3.3.4 | Raman spectroscopy | 67 |
| 3.3.5 | X-ray photoelectron spectroscopy | 67 |
| 3.3.6 | Fourier-transform infrared spectroscopy | 67 |
| 3.3.7 | Physisorption of Nitrogen at 77 K | 68 |
| 3.3.8 | Thermogravimetric analysis | 68 |
| 3.3.9 | Visual observation | 68 |
| 3.3.10 | Zeta potential analysis | 69 |
| 3.3.11 | Ultraviolet-visible spectrophotometer | 69 |
| 3.3.12 | Viscosity | 70 |
| 3.3.13 | Measurement of contact angle | 70 |
| 3.3.14 | Electrical conductivity | 71 |
| 3.3.15 | Mechanical properties..... | 72 |
| CHAPTER 4 RESULTS AND DISCUSSION | | 74 |
| 4.1 | Properties of graphene foam and commercial graphene-based materials | 74 |
| 4.1.1 | Morphology | 75 |
| 4.1.2 | X-ray diffraction analysis | 81 |
| 4.1.3 | Fourier-transform infrared spectroscopy analysis | 84 |
| 4.1.4 | Raman spectroscopy analysis | 85 |
| 4.1.5 | X-ray photoelectron spectroscopy analysis | 87 |
| 4.1.6 | Thermal properties..... | 91 |
| 4.2 | Properties of graphene-based materials mixed with polyester varnish binder..... | 93 |
| 4.2.1 | Visual observation | 93 |
| 4.2.2 | Viscosity analysis | 94 |

| | | |
|--|---|------------|
| 4.2.3 | Surface wettability analysis | 98 |
| 4.2.4 | Electrical conductivity properties | 101 |
| 4.3 | Properties of graphene-based inks..... | 106 |
| 4.3.1 | Effect of GNPs dispersed in various types of common solvents.... | 107 |
| 4.3.1(a) | Visual observation | 107 |
| 4.3.1(b) | Zeta potential analysis | 110 |
| 4.3.1(c) | UV-Vis spectrophotometer analysis | 111 |
| 4.3.1(d) | Viscosity analysis | 114 |
| 4.3.1(e) | Surface wettability analysis | 116 |
| 4.3.2 | Effect of GNPs and GF dispersed in mixed solvents | 119 |
| 4.3.2(a) | Visual observation | 119 |
| 4.3.2(b) | Zeta potential analysis | 121 |
| 4.3.2(c) | UV-Vis spectrophotometer analysis | 122 |
| 4.3.2(d) | Viscosity analysis | 124 |
| 4.3.2(e) | Surface wettability analysis | 125 |
| 4.3.2(f) | Morphology | 126 |
| 4.4 | Properties of graphene-based ink and graphene hybrid-based inks | 129 |
| 4.4.1 | Stability of GF ink, GF/AgNPs and GF/PEDOT:PSS hybrid inks. | 129 |
| 4.4.2 | Physical properties of GF ink, GF/AgNPs and GF/PEDOT:PSS hybrid inks | 134 |
| 4.4.3 | Properties of printed GF ink and GF hybrid inks | 136 |
| 4.4.4 | Properties of printed GF/PEDOT:PSS hybrid ink for strain sensor | 141 |
| CHAPTER 5 CONCLUSIONS AND FUTURE RECOMMENDATIONS .. | | 144 |
| 5.1 | Conclusions | 144 |
| 5.2 | Recommendations for future research..... | 145 |
| REFERENCES..... | | 147 |
| LIST OF PUBLICATIONS | | |

LIST OF TABLES

| | Page |
|---|------|
| Table 2.1 Chemical properties of common solvents used for graphene ink dispersion (Materials Safety Data Sheet; DataPhysics Instruments GmbH)..... | 12 |
| Table 2.2 Comparison of graphene-like materials terms (Bianco <i>et al.</i> , 2013)..... | 13 |
| Table 2.3 Comparison of the various types of graphene inks and electrical conductivity from literature (Huang <i>et al.</i> , 2011; Secor <i>et al.</i> , 2013; Gao <i>et al.</i> , 2014, Secor <i>et al.</i> , 2015; Miao <i>et al.</i> , 2016, Majee <i>et al.</i> , 2017; Secor <i>et al.</i> , 2017) | 20 |
| Table 2.4 Comparison of several types of conductive materials-based inks (Kordás <i>et al.</i> , 2006; Lee <i>et al.</i> , 2008; Kang <i>et al.</i> , 2010; Cui <i>et al.</i> , 2010; Nie <i>et al.</i> , 2012; Perinka <i>et al.</i> , 2013; Zhang <i>et al.</i> , 2015; Kastner <i>et al.</i> , 2017)..... | 24 |
| Table 2.5 Comparison of viscosity and surface tension of various types of conductive inks from literature (Wu <i>et al.</i> , 2009; Jeong <i>et al.</i> , 2011; Denneulin <i>et al.</i> , 2011; Vaseem <i>et al.</i> , 2012; Öhlund <i>et al.</i> , 2012; Capasso <i>et al.</i> , 2015; Deng <i>et al.</i> , 2017) | 32 |
| Table 2.6 Performances of flexible graphene-based strain sensors (Eswaraiah <i>et al.</i> , 2011; Wang <i>et al.</i> , 2013; Filippidou <i>et al.</i> , 2015; Liu <i>et al.</i> , 2016; Lin <i>et al.</i> , 2016; Chun <i>et al.</i> , 2017; Zhang <i>et al.</i> , 2019)..... | 49 |
| Table 3.1 General properties of various types of graphene-like materials (Materials Safety Data Sheet) | 53 |
| Table 3.2 General properties of silver nanoparticles (Materials Safety Data Sheet) | 54 |
| Table 3.3 General properties of PEDOT:PSS (Materials Safety Data Sheet)..... | 54 |
| Table 3.4 General properties of PV (Materials Safety Data Sheet) | 55 |

| | |
|---|-----|
| Table 3.5 General properties and chemical formula of various types of solvents and chemicals (Materials Safety Data Sheet)..... | 56 |
| Table 3.6 Description of the sample codes for GNPs and GF dispersed into various ratios of IPA:EG mixed solvents..... | 63 |
| Table 4.1 Average lateral size, BET surface area and pore volume of the graphene-based materials..... | 78 |
| Table 4.2 The crystallite size (L_c), interlayer distance (d) and number of layers (n) of the graphene-based materials..... | 84 |
| Table 4.3 Raman intensity of the graphene-based materials..... | 87 |
| Table 4.4 The elemental compositions of carbon (C 1s), oxygen (O 1s) and O/C atomic ratio of the graphene-based materials..... | 90 |
| Table 4.5 Decomposition temperature and weight of residue of the graphene-based materials..... | 92 |
| Table 4.6 Comparison of the maximum electrical conductivity and percolation threshold between present study and graphene-filled polymer from literature (Hu <i>et al.</i> , 2012; Wang <i>et al.</i> , 2015; Chiu <i>et al.</i> , 2016; Alam <i>et al.</i> , 2016; Ma <i>et al.</i> , 2017; Wang <i>et al.</i> , 2018; Jun <i>et al.</i> , 2018) | 105 |
| Table 4.7 General properties of various types of solvents (Hernandez <i>et al.</i> , 2010; Johnson <i>et al.</i> , 2015) | 109 |
| Table 4.8 Viscosity of solvents and GNPs dispersed in various types of solvents . | 114 |
| Table 4.9 Comparison properties of GNPs dispersed in various types of solvents. | 119 |
| Table 4.10 Viscosity of mixed solvent and viscosity of GNPs and GF in various ratios of IPA:EG mixed solvents..... | 124 |
| Table 4.11 Comparison properties of GNPs and GF in various ratios of IPA:EG mixed solvents..... | 128 |
| Table 4.12 Concentration decrement and zeta potential of GF and GF hybrid inks | 134 |
| Table 4.13 Comparison physical properties of GF and GF hybrid inks..... | 135 |

Table 4.14 Comparison of gauge factor between present study and from literature

.....143

LIST OF FIGURES

| | Page |
|---|------|
| Figure 1.1 The number of published papers for conductive inks 2009-2018 from Scopus by searching for the topic “conductive ink” (data acquired on October 2019)..... | 3 |
| Figure 1.2 Market value share (million USD) for conductive inks in emerging sectors 2016-2026 (Zervos, 2016)..... | 4 |
| Figure 2.1 Schematic of (a) coffee-ring effect at low drying temperature and (b) surface capture effect at high drying temperature (Li <i>et al.</i> , 2016).... | 11 |
| Figure 2.2 Comparison of quality against price (for mass production) for graphene elaboration methods (Novoselov <i>et al.</i> , 2012)..... | 16 |
| Figure 2.3 SEM images of graphene foam (GF) (Liu <i>et al.</i> , 2014)..... | 16 |
| Figure 2.4 (a) Photograph of a printed pattern on PI substrate and (b) the electrical conductivity of the printed patterns on PI (Huang <i>et al.</i> , 2011)..... | 17 |
| Figure 2.5 (a) Schematic experimental setup for the electrochemical exfoliation process, photo pictures of (b) electrochemical-GNPs ink ready for inkjet printing, (c) printed patterns on a plastic substrate and (d) printed test sample on a glass substrate, and (e) variations of sheet resistance and optical transmittance with number of prints at different annealing temperatures (Miao <i>et al.</i> , 2016)..... | 19 |
| Figure 2.6 (a) The route to synthesize Ag/rGO composite by reducing both the Ag and GO, (b) different patterns obtained by inkjet printing on office paper, (c) conductive tracks in different width on PET for circuit test and (d) surface resistance and the surface morphology of the printed conductive tracks (Zhang <i>et al.</i> , 2016) | 26 |
| Figure 2.7 Viscosity curves of graphene ink with dispersing agent at various temperatures (Dybowska-Sarapuk <i>et al.</i> , 2018)..... | 28 |
| Figure 2.8 Schematic of (a) surface tension from intermolecular forces, (b) droplet onto substrate surface with an ideal contact angle (θ_c), and | |

| | |
|---|----|
| comparison of droplet shapes with (c) high surface energy and (d) low surface energy on the substrates..... | 30 |
| Figure 2.9 Schematic of wetting behaviors of a droplet onto substrate surface at different contact angles (θ_{eq}) | 31 |
| Figure 2.10 Plot of surface tension (20 °C) of (a) GO dispersion and (b) GO/SDS hybrid dispersion varied with dispersion concentration (Li <i>et al.</i> , 2018) | 32 |
| Figure 2.11 UV spectra of graphene and GO (Johra <i>et al.</i> , 2014) | 35 |
| Figure 2.12 Schematic of the ζ potential double layer model for a negatively charged graphene sheet (Johnson <i>et al.</i> , 2015) | 37 |
| Figure 2.13 Zeta potentials of graphene dispersions against donor number (blue, shaded square) and acceptor numbers (red, open square)..... | 37 |
| Figure 2.14 Recent developments in the field of flexible electronics; (a) stretchable strain sensor, (b) flexible circuit film (Penn State, 2013; Diabetes Queensland, 2017)..... | 39 |
| Figure 2.15 Schematic of the screen printing process (Gonzalez-Macia <i>et al.</i> , 2010) | 41 |
| Figure 2.16 Schematic of an air pressure spray coating process (Zabihi <i>et al.</i> , 2015) | 42 |
| Figure 2.17 (a) Schematic of the spray coating process and (b) optical transmittance as a function of the sheet resistance (Carey <i>et al.</i> , 2018) | 43 |
| Figure 2.18 Schematic of inkjet printing (a) continuous inkjet system and (b) on-demand inkjet system (Lau and Shrestha, 2017) | 44 |
| Figure 2.19 The number of published papers for flexible strain sensors 2009-2018 from Scopus by searching for the topic “flexible strain sensors” (data acquired on October 2019)..... | 46 |
| Figure 2.20 Schematic of the strain sensor gauge (Correia <i>et al.</i> , 2013) | 48 |
| Figure 3.1 Overall research flowchart..... | 58 |

| | |
|--|----|
| Figure 3.2 (a) Solvothermal reaction to produce sodium ethoxide, (b) pyrolysis reaction for producing graphene foam, (c) washing and filtration of pyrolysis products, (d) sodium ethoxide and (e) product of pyrolysis | 59 |
| Figure 3.3 Photograph of the customized motor-controlled air spray coating..... | 61 |
| Figure 3.4 Schematic of the fabrication process of conductive ink pattern using spray coating technique..... | 61 |
| Figure 3.5 Photograph of the inkjet printing | 64 |
| Figure 3.6 Schematic of the fabrication process of conductive ink pattern using inkjet printing technique | 64 |
| Figure 3.7 The principle of Van der Pauw's measurement..... | 72 |
| Figure 4.1 SEM micrographs of (a) GF, (c) GNPs and (e) SG particles [1000X mag.], the inset is an image of porous GF at 2000X mag., EDS analysis of (b) GF, (d) GNPs and (f) SG particles | 76 |
| Figure 4.2 Lateral size distribution histogram measured by ImageJ of (a) GF,..... | 77 |
| Figure 4.3 HRTEM micrographs of (a, b) GF, (c, d) GNPs and (e, f) SG particles at magnifications of (a, c, e) 97kX and (b, d, f) 690 kX | 79 |
| Figure 4.4 SAED of (a) GF, (b) GNPs and (c) SG particles | 80 |
| Figure 4.5 XRD patterns of (a) GF, (b) GNPs and (c) SG particles | 82 |
| Figure 4.6 FTIR spectra of (a) GF, (b) GNPs and (c) SG particles | 85 |
| Figure 4.7 Raman spectra of (a) GF, (b) GNPs and (c) SG particles..... | 87 |
| Figure 4.8 XPS spectra of (a) GF, (b) GNPs and (c) SG particles..... | 89 |
| Figure 4.9 C 1s spectra band highlighted of (a) GF, (b) GNPs and (c) SG particles | 90 |
| Figure 4.10 Weight loss (solid line) and derivative weight loss (dotted line) of (a) GF, (b) GNPs and (c) SG particles with respect to temperature..... | 92 |
| Figure 4.11 Photographs of (a, d) GNPs ink, (b, e) SG ink and (c, f) GF ink were observed at (a-c) before sonication and (d-f) after sonication | 93 |

| | |
|---|-----|
| Figure 4.12 (a) Viscosity curves of conductive inks at 5 vol.% as a function of shear rate, (b) viscosity variation as a function of filler loadings at 500 s ⁻¹ shear rate, and viscosity curves of (c) GNPs ink, (d) SG ink and (e) GF ink with fitted Carreau Model curve..... | 95 |
| Figure 4.13 Illustration of contact angle measurement (example: 1 vol.% GF ink) when: (a) drop falling and (b) as the drop settled on the surface of the substrate, (c) contact angle variation as a function of filler loadings, inset showing (i) small and (ii) high contact angle..... | 99 |
| Figure 4.14 Surface energy as a function of filler loadings including Young's equation | 100 |
| Figure 4.15 Electrical conductivity of (a) GF ink, (b) GNPs ink and (c) SG ink as a function of filler loading, inset showing digital images of an electronic circuit set up and LED brightness for various types of conductive ink patterns at 10 vol. % | 103 |
| Figure 4.16 SEM micrographs of cross-section conductive ink patterns made of (a) 7 vol.% GF (b) 12 vol.% GF, (c) 2 vol.% GNPs (d) 4.5 vol.% GNPs (e) 9 vol.% SG [2,500-3,500X mag.] | 104 |
| Figure 4.17 Photographs of GNPs dispersed in (a) EG, (b) PG, (c) IPA, (d) NMP and (e) DMF. Figure (i), (ii) and (iii) refer to the image after sonication (day 1), day 3 and day 7, respectively | 108 |
| Figure 4.18 Schematic of GNPs dispersed in solvent after a period of time | 109 |
| Figure 4.19 Zeta potentials of GNPs dispersed in various types of solvents | 111 |
| Figure 4.20 UV-Vis absorption spectra of GNPs dispersed in various types of solvents at different periods of time..... | 113 |
| Figure 4.21 Concentration of GNPs dispersed in various types of solvents as a function of time | 113 |
| Figure 4.22 Viscosity curves of GNPs dispersed in (a) PG, (b) EG, (c) NMP, (d) IPA and (e) DMF solvents as a function of shear rate | 116 |
| Figure 4.23 Contact angle of GNPs dispersed in various types of solvents, inset showing the drop settled on the surface of the substrate..... | 117 |

| | |
|--|-----|
| Figure 4.24 Surface energy of GNPs dispersed in various types of solvents, inset showing a contact angle including Young's equation..... | 118 |
| Figure 4.25 Photographs of (a-c) GNPs and (d-f) GF in various ratios of IPA:EG mixed solvents. Figure (a, d) IPA:4EG, (b, e) IPA:EG and (c, f) 4IPA:EG refer to the image after sonication (day 1), day 3 and day 7, respectively | 120 |
| Figure 4.26 Zeta potentials of GNPs and GF dispersed in various ratios of IPA:EG mixed solvents..... | 121 |
| Figure 4.27 UV-Vis absorption spectra of GNPs inks and GF inks in IPA:EG solvent at different periods of time | 123 |
| Figure 4.28 Concentration of GNPs inks and GF inks in various ratios of IPA:EG mixed solvents as a function of time..... | 123 |
| Figure 4.29 Contact angle and surface energy of GNPs and GF in various ratios of IPA:EG mixed solvents | 126 |
| Figure 4.30 The droplet of (a) GNPs inks and (b) GF inks at various ratios of IPA:EG mixed solvents (i) 1:4, (ii) 2:3, (iii) 1:1, (iv) 3:2 and (v) 4:1 on PET substrate | 126 |
| Figure 4.31 HRTEM micrographs of GF particles in IPA:EG mixed solvents at 1:1 ratio at magnifications of (i, iii) 15kX and (ii, iv) 690kX. Figure (i-ii) and (iii-iv) refer to the image after sonication (day 1) and day 5, respectively | 127 |
| Figure 4.32 Photographs of (a) GF ink, (b) GF/AgNPs hybrid ink and (c) GF/PEDOT:PSS hybrid ink. Figure (i), (ii) and (iii) refer to the image after sonication (day 1), day 3 and day 7, respectively | 130 |
| Figure 4.33 UV-Vis absorption spectra of (a) GF, (b) GF/AgNPs hybrid ink and (c) GF/PEDOT:PSS hybrid ink | 132 |
| Figure 4.34 Concentration of GF ink, GF/AgNPs hybrid ink and GF/PEDOT:PSS hybrid ink as a function of time | 133 |
| Figure 4.35 Viscosity curves of (a) GF ink, (b) GF/PEDOT:PSS hybrid ink and (c) GF/AgNPs hybrid ink as a function of shear rate..... | 135 |

| | | |
|--------------------|---|-----|
| Figure 4.36 | The droplet of (a) GF ink, (b) GF/AgNPs hybrid ink and | 136 |
| Figure 4.37 | Photographs of printed (a) GF ink, (b) GF/AgNPs hybrid ink and (c) GF/PEDOT:PSS hybrid ink on PET substrate with different printing layers (i) 10 layers, (ii) 20 layers, (iii) 30 layers, (iv) 40 layers and (v) 50 layers | 137 |
| Figure 4.38 | (a) Surface conductivity of GF ink and GF hybrid inks as a function of printing layer and (b) enlargement of surface conductivity of GF ink and GF/AgNPs hybrid ink, inset showing digital images of an electronic circuit set up and LED brightness for printed GF ink and GF hybrid inks..... | 138 |
| Figure 4.39 | Photographs of ink cartridge problems due to poor stability including (a) nozzle clogged and (b) conductive ink trapped on the ink cartridge filter; in comparison with (c) no conductive material trapped on the cartridge filter | 139 |
| Figure 4.40 | SEM micrographs of top printed surface made of (a, b) GF ink, (c,d) GF/AgNPs hybrid ink and (e, f) GF/PEDOT:PSS hybrid ink at (a), (c), (e) 10 printing layers and (b), (d), (f) 50 printing layers [100X mag.]..... | 140 |
| Figure 4.41 | Relative change resistance and hysteresis behavior of GF/PEDOT:PSS hybrid sensor as a function of strain, inset showing digital image of an tensile test set up for printed GF/PEDOT:PSS hybrid sensor | 142 |

LIST OF SYMBOLS

| | |
|------------|------------------------|
| m | Metre |
| % | Percentage |
| J | Joule |
| g | Gram |
| °C | Degree Celsius |
| L | Litre |
| V | Volt |
| W | Watt |
| Pa | Pascal |
| N | Newton |
| S | Siemens |
| Ω | Ohm |
| sq | Square |
| min | Minutes |
| h | Hour |
| S | Siemens |
| s | Second |
| η | Viscosity |
| γ | Surface energy |
| θ_c | Contact angle |
| P | Poise |
| π | Pi |
| ζ | Zeta potential |
| Hz | Hertz |
| vol.% | Volume percent |
| psi | Pounds per square inch |
| θ | Theta |
| λ | Wavelength |
| Å | Angstrom |
| ° | Degree |

| | |
|----------|---------------------|
| eV | Electronvolt |
| ρ | Resistivity |
| σ | Conductivity |
| t | Thickness |
| R | Sheet resistance |
| f | Correction factor |
| L | Length |
| a.u. | Arbitrary unit |
| d | Interlayer distance |
| L_c | Crystallite size |
| k | Constant |
| wt.% | Weight percent |

LIST OF ABBREVIATIONS

| | |
|-------|---|
| 2D | Two-dimensional |
| GNPs | Graphite nanoplatelets |
| GO | Graphene oxide |
| CVD | Chemical vapor deposition |
| LPE | Liquid phase exfoliation |
| RGO | Reduced graphene oxide |
| GF | Graphene foam |
| AuNPs | Gold nanoparticles |
| AgNPs | Silver nanoparticles |
| CuNPs | Copper nanoparticles |
| 3D | Three-dimensional |
| NMP | N-Methyl-2-pyrrolidone |
| DMSO | Dimethylsulfoxide |
| DMF | N,N-Dimethylformamide |
| IPA | 2-propanol |
| EG | Ethylene glycol |
| PG | Propylene glycol |
| SG | Synthetic graphite |
| PV | Polyester varnish |
| PET | Polyethylene terephthalate |
| SEM | Scanning electron microscopy |
| EDS | Energy dispersive spectroscopy |
| HRTEM | High resolution transmission electron microscopy |
| XRD | X-ray diffraction |
| XPS | X-ray photoelectron spectroscopy |
| FTIR | Fourier-transform infrared spectroscopy |
| BET | Brunauer-emmett-teller |
| TGA | Thermogravimetric analysis |
| THF | Tetrahydrofuran |

| | |
|-----------|---|
| PI | Polyimide |
| FGO | Few-layered graphene oxide |
| PEN | Poly(ethylenephthalate) |
| CNTs | Carbon nanotubes |
| PANI | Polyaniline |
| PPy | Polypyrrole |
| PEDOT:PSS | Poly(3,4-ethylenedioxythiophene)- poly(styrenesulfonate) |
| MWCNT | Multi-walled carbon nanotube |
| SWCNT | Single-walled carbon nanotube |
| PDMS | Polydimethylsiloxane |
| PVDF | Polyvinylidene fluoride |
| TPU | Thermoplastic polyurethane |
| SAED | Selected area electron diffraction |
| FWHM | Full-width at half maximum |

FABRIKASI DAN PENCIRIAN DAKWAT BERASASKAN GRAFEN

ABSTRAK

Tujuan utama kajian ini dijalankan adalah untuk membangunkan dakwat berasaskan grafen dengan kestabilan, sifat-sifat elektronik dan fizikal yang baik untuk percetakan elektronik dengan menggunakan teknologi salutan semburan dan percetakan inkjet. Pertama, perbandingan untuk bahan seperti-grafen yang berbeza menunjukkan bahawa busa grafen (GF) mempamerkan permukaan yang tertinggi dengan nilai $2136 \text{ m}^2\text{g}^{-1}$. Sementara itu, grafit nanoplatlet (GNPs) dan grafit sintetik (SG) mempamerkan struktur hablur yang tinggi dengan kewujudan puncak (002) yang tajam dan sempit, dan zarah yang berkualiti tinggi dengan nisbah I_D/I_G yang rendah. Kedua, keputusan menunjukkan bahawa kelikatan dan sudut sentuhan dakwat yang konduktif meningkat dengan ketara dengan penambahan pengisian GF, GNPs dan SG dalam penguat varnis poliester (PV). Penambahan 10% isipadu GNPs meningkatkan konduktiviti elektrik PV sebanyak 186 %, dan hanya 40 % untuk SG dan 10 % untuk GF pada jumlah pengisi yang sama. Seterusnya, didapati bahawa GNPs disebar di dalam glikol etilena (EG) mempamerkan kestabilan yang baik dengan penurunan sebanyak 85% daripada kepekatan awal selepas sebulan, kelikatan dan kebolehbasahan berbanding glikol propilena (PG) dan 2-propanol (IPA). Selain itu, GF disebar di dalam pelarut campuran IPA:EG pada nisbah 1:1 menunjukkan penurunan sebanyak 50 % sahaja daripada kepekatan awal selepas sebulan berbanding dengan dakwat GNPs pada nisbah campuran yang sama. Untuk bahagian akhir, dakwat GF, dakwat hibrid GF/poli(3,4-etilenadioksitiofena) poli(stirenasulfonat) (PEDOT:PSS) menunjukkan kestabilan yang baik berbanding dakwat GF dan dakwat hibrid GF/nanopartikel perak (AgNPs) di mana dakwat menunjukkan penurunan kepekatan sebanyak 30 % selepas sebulan, peningkatan kekonduksian permukaan sebanyak 100 % pada 50 lapisan cetakan dan

faktor tolok sebanyak 4.3. Kesimpulannya, hibrid GF/PEDOT:PSS yang bercetak mempunyai potensi untuk digunakan sebagai aplikasi sensor regangan.

FABRICATION AND CHARACTERIZATION OF GRAPHENE-BASED INK

ABSTRACT

The main aim of the present study is to develop graphene-based ink with excellent stability, electrical and physical properties for printing electronics by utilizing spray coating and inkjet printing techniques. Firstly, comparison on the different types of graphene-like materials showed that graphene foam (GF) exhibited the highest surface area with the value of $2136 \text{ m}^2\text{g}^{-1}$. Meanwhile, graphite nanoplatelets (GNPs) and synthetic graphite (SG) displayed highly crystalline structures with the presence of sharp and narrow (002) peak, and high-quality particles with lower I_D/I_G ratio. Secondly, results showed that viscosity and contact angle of the conductive inks increased significantly with increasing GF, GNPs and SG filler loadings in a polyester varnish (PV) binder. The incorporation of 10 vol.% GNPs improved the electrical conductivity of PV by 186 %, and only 40 % for SG and 10 % for GF at the same filler loading. Next, it is found that GNPs dispersed in ethylene glycol (EG) exhibited better stability with 85 % decrement of the initial concentration after a month, viscosity and wettability than those of propylene glycol (PG) and 2-propanol (IPA). On the other hand, GF dispersed in IPA:EG mixed solvent at ratio of 1:1 showed only 50 % decrement from the initial concentration after a month compared to those of GNPs inks at the same mixed ratio. In the last part, GF/poly(3,4-ethylenedioxythiophene) poly(styrenesulfonate) (PEDOT:PSS) hybrid ink exhibited better stability than GF ink and GF/silver nanoparticles (AgNPs) hybrid ink where the ink showed 30 % decrement from the concentration after a month, 100 % improvement in surface conductivity at 50 printed layers and gauge factor of 4.3. As a conclusion, printed GF/PEDOT:PSS hybrid ink has the potential to be used for strain sensor applications.

FABRICATION ET CARACTERISATION DE L'ENCRE A BASE DE GRAPHENE

RÉSUMÉ

L'objectif principal de la présente étude est de développer des encres à base de graphène présentant d'excellentes propriétés de stabilité, électriques et physiques pour l'électronique d'impression en utilisant des techniques de revêtement par pulvérisation et d'impression par jet d'encre. Premièrement, la comparaison des différents types de matériaux similaires au graphène a montré que la mousse de graphène (GF) présentait la plus grande surface spécifique avec une valeur de $2136 \text{ m}^2\text{g}^{-1}$. Par ailleurs, les nanoplaquettes de graphite (GNPs) et le graphite synthétique (SG) présentaient des structures hautement cristallines avec la présence d'un pic aigu et étroit (002) et de particules de haute qualité avec un rapport I_D/I_G inférieur. Deuxièmement, les résultats ont montré que la viscosité et l'angle de contact des encres conductrices augmentaient significativement avec l'augmentation des charges de GF, GNPs et SG dans un liant de vernis polyester (PV). L'incorporation de 10 % en volume de PNB a amélioré la conductivité électrique du PV de 186 %, et seulement 40 % pour la SG et 10 % pour le GF avec la même charge de remplissage. Ensuite, il a été constaté que les PNB dispersés dans l'éthylène glycol (EG) présentaient une meilleure stabilité avec une diminution de 85% de la concentration initiale après un mois, une viscosité et une mouillabilité supérieures à celles du propylène glycol (PG) et du 2-propanol (IPA). D'autre part, le GF dispersé dans un solvant mélangé IPA:EG avec un rapport de 1:1 n'a montré qu'une diminution de 50 % par rapport à la concentration initiale après un mois comparant à ceux des encres GNP dans le même rapport de mélange. Dans la dernière partie, l'encre hybride GF/poly(3,4-éthylènedioxythiophène) poly(styrène-sulfonate) (PEDOT:PSS) a montré une meilleure stabilité que l'encre hybride GF et

l'encre hybride GF/nanoparticules d'argent (AgNPs) où l'encre a montré 30 % de réduction de concentration après un mois, 100 % d'amélioration en termes de conductivité superficielle à 50 couches imprimées et un facteur de gauge de 4.3. En conclusion, l'encre hybride imprimée GF/PEDOT:PSS a le potentiel d'être utilisée pour les applications de capteurs de contrainte.

CHAPTER 1

INTRODUCTION

1.1 Background

Recent years have witnessed a revolution in graphene due to its distinctive physicochemical properties, tremendous mechanical performance and its unique electrical and thermal conductivities (Novoselov *et al.*, 2004). Presently, graphene has been widely used in various electronic applications including as the conductive inks for printable flexible electronics. Graphene expression consists of a prefix of “*graph*” from graphite and suffix “*ene*” from C-C double bonds (Bianco *et al.*, 2013; Ghany *et al.*, 2017). Graphene by definition is a single atomic layer of carbon atoms packed into two-dimensional (2D) honeycomb lattice structure. The atoms are arranged in hexagonal structure creating a sheet of sp^2 tightly bonded carbon. Graphene has been considered as “the thinnest, most flexible and strongest material known” that conducts heat and electricity very well (Jaworski *et al.*, 2013; Brownson and Banks, 2014). The thickness (number of layers) in 2D carbons goes from 0.34 nm (monolayer graphene) up to several micrometers. In 1947, Wallace in his study has explained that almost all ‘graphene-like materials’ are different from the idealized 2D ‘graphene structure’. Several types of graphene-like materials had been existing from monolayer to multilayer graphene, turbostratic carbon, graphite nanoplatelets (GNPs), graphene foam (GF) and graphene oxide (GO) (Choucair *et al.*, 2009; Bianco *et al.*, 2013).

To date, several methods for the mass production of graphene have been explored including chemical vapor deposition (CVD), liquid phase exfoliation (LPE), graphite oxide route leading to graphene oxide (GO) or reduced graphene oxide (RGO), electrochemical route and solvothermal method (Chen *et al.*, 2004; Choucair

et al., 2009; Novoselov *et al.*, 2012; Low *et al.*, 2013, Speyer *et al.*, 2015). Among these methods, LPE method is considered one of the simplest methods and yields larger quantities of graphene, however the number of graphene layers is inconsistent as the layers may reaggregate and this method introduces chemical and physical defects in the graphene layers, which may not be suitable to be used as conductive inks (Parvez *et al.*, 2015). Choucair *et al.* (2009) reported that solvothermal method is an alternative bottom-up approach for the production of graphene-like materials, low cost of raw materials, has the ability to yield graphene in large scale, etc. According to Ma *et al.* (2014) and Speyer *et al.* (2015), solvothermal reaction method has been widely studied previously for the production of graphene foam (GF).

Conductive ink made of graphene has become a topic of interest due to its superior electrical properties in comparison of various conductive nanomaterials, conductive polymers and other carbon-based materials while at the same time reducing production costs (Arapov *et al.*, 2014). An ideal conductive ink should be inexpensive, simple preparation, good printability, low viscosity, good stability, good adhesion to the substrate and high electrical conductivity values even after printing (Choi *et al.*, 2015; Liu *et al.*, 2015; Stoppa and Chiolerio, 2014). According to the statistic of scientific journals related to conductive inks which were taken from Scopus as in Figure 1.1, it shows that the number of scientific publications exhibited 416% improvement specifically from 2009 to 2018.

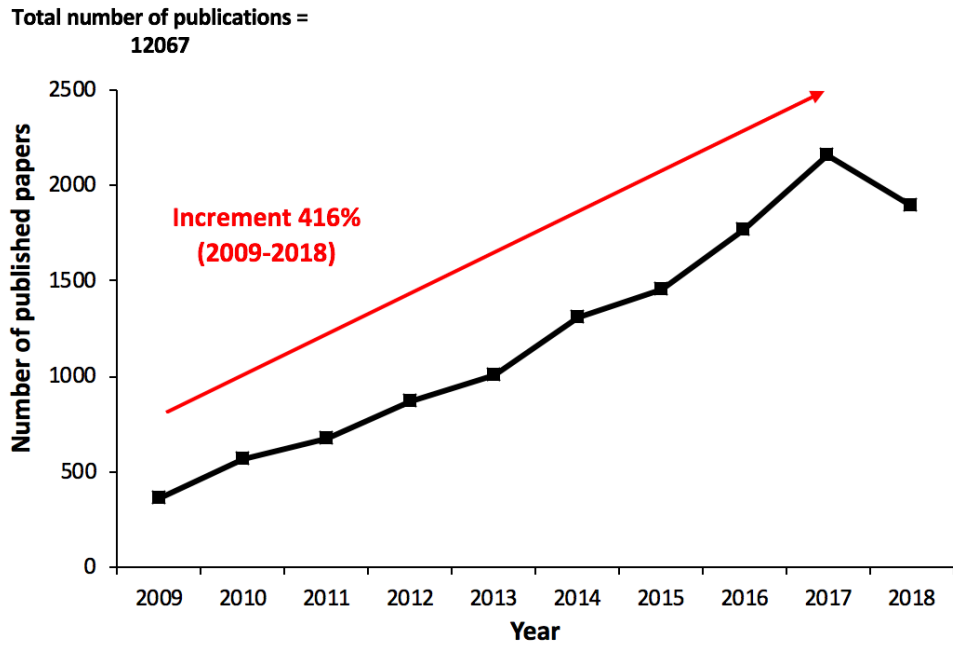


Figure 1.1 The number of published papers for conductive inks 2009-2018 from Scopus by searching for the topic “conductive ink” (data acquired on October 2019)

Furthermore, conductive ink is one of the main elements in the printing industry such as inkjet printing, spray coating, screen printing, etc for flexible electronic applications. Figure 1.2 illustrates the market value share for conductive inks in printed electronic applications including organic light-emitting diode (OLED), organic and inorganic photovoltaics, flexible displays, radio-frequency identification (RFID), healthcare devices, thin film transistor, solar cells, sensors, smart textiles, batteries, memories, and antenna (Capasso *et al.*, 2015; Suganuma, 2014; Denneulin *et al.*, 2011; Kamyshny and Magdassi, 2014; Li *et al.*, 2010). The market value share for conductive inks is expected to increase gradually up to 2026.

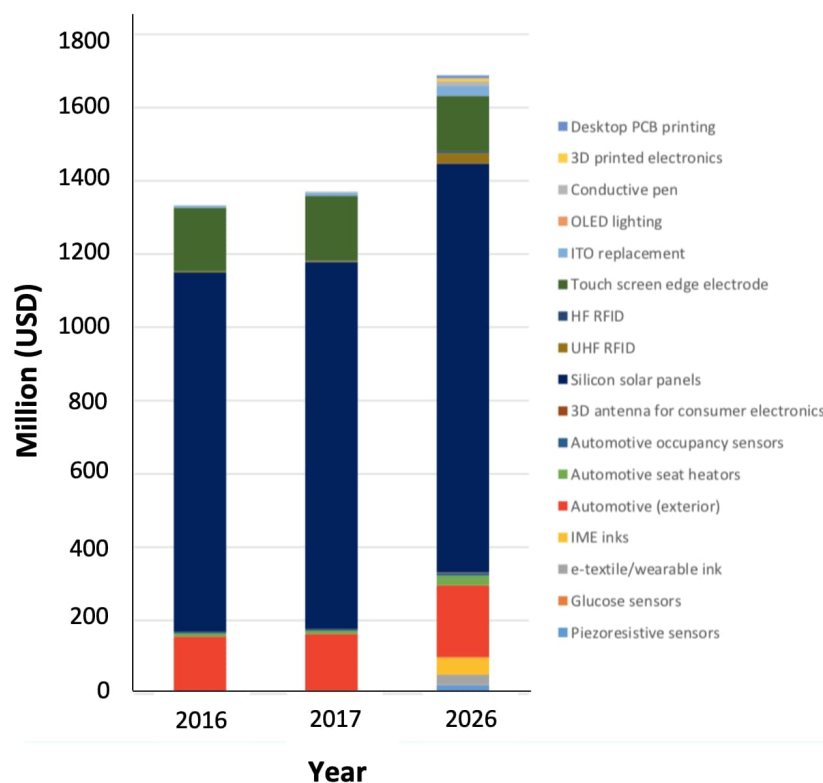


Figure 1.2 Market value share (million USD) for conductive inks in emerging sectors 2016-2026 (Zervos, 2016)

1.2 Problem statements

Numerous researches of the conductive nanomaterials and conductive polymer inks have been done for the production of printed electronic applications. Among them, metal-based inks such as gold nanoparticles (AuNPs), silver nanoparticles (AgNPs) and copper nanoparticles (CuNPs) have received a great attention due to their excellent electrical conductivity. AuNPs and AgNPs suffer from high cost and require high sintering temperature which limiting their functions to be used with flexible substrates (Cui *et al.*, 2010; Nie *et al.*, 2012; Kastner *et al.*, 2017), making CuNPs a good alternative due to the low cost and high electrical conductivity. However, CuNPs have issues with oxidation under heat and humidity conditions which limits its applications (Kang *et al.*, 2010). Meanwhile for conductive polymers, the electrical

conductivity is still considered to be very low as compared to those of metal-based inks (Perinka *et al.*, 2013). Due to that, considering the advantages of graphene over other conductive nanoparticles and conductive polymers, graphene-based inks have been widely explored since the past 10 years (Cheng *et al.*, 2017; Tran *et al.*, 2018), however more effort still need to be considered before they can be used in practical applications. Extensive works to produce good quality graphene-based inks are required. Ink formulation and properties mainly influence the printing quality and it must be optimized in order to achieve patterns without a coffee ring effect and homogeneity of the printed patterns.

Most of the graphene-based inks reported in the literature were prepared by utilizing GNPs and GO as the fillers. Due to the nature of graphene which is hydrophobic, it is very difficult to achieve stable dispersions in various types of common solvents. Addition of surfactant in the conductive ink is required to improve the solubility of the conductive ink, however it reduces the conductivity value. Meanwhile, GO suffer from low electrical conductivity due to the high oxygen-based functional groups content (around 8%). Therefore, reduction process is important to remove the functional groups, however this process involves highly toxic materials which is not environmentally friendly and introduced defects which compromise the conductivity value (Pei and Cheng, 2012). Due to that, alternative graphene-like material which has good electrical properties and quality is preferred to be used in the preparation of conductive ink. Based on the literature studies, reports on utilizing graphene foam (GF) produced by using solvothermal reaction method for conductive ink are very limited. According to Salunkhe *et al.* (2016), Tang *et al.* (2016) and Ma *et al.* (2017), the unique structure of GF which is constructed of three-dimensional (3D) interconnected network with very high surface area to avoid aggregation yet

maintaining the electrical conductivity can be considered to be explored for the fabrication of graphene-based conductive ink.

Coleman (2013) and Nicolosi *et al.* (2013) reported that most of graphene-based inks were produced by using effective solvents such as N-Methyl-2-pyrrolidone (NMP), Dimethylsulfoxide (DMSO) and N,N-Dimethylformamide (DMF) due to the surface tension that is closed to 40 mJm^{-2} . However, these solvents suffer from highly toxic especially for women which may damage fertility or the unborn child (hazard code = H360) (Byrne et al. 2016). In addition, these solvents have high boiling points ($>150 \text{ }^\circ\text{C}$) which are not suitable to be used with plastic substrates, that require low processing temperature. Alternative solvents with low boiling points, less toxic and high surface tension are preferred in the preparation of good dispersion conductive ink. Acetone, 2-propanol (IPA) and ethanol are some of the common alternative solvents that have low boiling points, however these solvents exhibit low surface tension approximately 23 mJm^{-2} , that lead to poor graphene dispersion (Tran *et al.*, 2018). From the literature review, reports on preparing graphene-based ink by using ethylene glycol (EG) and propylene glycol (PG) are limited. These solvents have surface tension close to 40 mJm^{-2} and are less toxic than NMP and DMF solvents, as reported by Byrne et al. (2016), but these solvents suffer from high boiling points. Therefore, it is expected that by mixing these solvents with other common solvents that have low boiling point, could produce graphene-based ink with excellent dispersion stability and physical properties.

Various printing techniques including screen printing, spray coating, 3D printing, inkjet printing, etc have been utilized in the fabrication of conductive ink patterns for various electronic applications (Khan *et al.*, 2015). Among these printing

techniques, spray coating and inkjet printing received more attentions due to the simple printing process, high repeatability, economical and save time compared to other printing techniques. However, these printing techniques often suffer from nozzle clogging due to the aggregation of the particles in the conductive inks. Thus, the ink properties such as viscosity, surface tension, contact angle and surface energy should be optimized to meet the specific printing requirements. Hoath (2016) reported that an ideal ink should possess low viscosity and high surface tension in order to flow through the nozzle easily without coagulate or stuck in the nozzle.

1.3 Objectives

The main objective of this research work is to produce graphene-based inks using alternative common solvents for printed electronics. In order to achieve it, the following steps are required:

1. To compare the characteristics of the synthesized graphene foam with commercial graphite nanoplatelets and synthetic graphite.
2. To investigate the ink properties of graphene-based materials mixed with polyester varnish binder and determine the electrical properties of the conductive ink patterns fabricated using spray coating technique.
3. To determine the dispersion stability and physical properties of graphite nanoplatelets and graphene foam dispersed into various types of common solvents and mixed solvents.
4. To identify the stability of graphene-based ink and graphene hybrid-based inks and investigate the electrical properties of the conductive ink patterns fabricated using inkjet printing technique.

1.4 Scope of study

This research has been devoted to produce graphene-based ink by using GF as novel material with surface area of 2000-2300 m²g⁻¹ which has been prepared via solvothermal reaction method. GNPs and synthetic graphite (SG) were also used in the preparation of graphene-based inks for comparison.

Two commonly printing techniques such as spray coating and inkjet printing were utilized in the fabrication of the printed patterns. The graphene-based materials were first mixed with polyester varnish (PV) binder and deposited onto a flexible substrate using a customized motor-controlled air spray coating. Secondly, GF and GNPs fillers were dispersed into various types of alternative less toxic solvents including EG, IPA and PG and also, the mixture of EG and IPA mixed solvents before being printed onto polyethylene terephthalate (PET) substrate via inkjet printing.

The characteristics of the synthesized GF and commercial GNPs and SG were examined by scanning electron microscopy (SEM), high resolution transmission electron microscopy (HRTEM), X-ray diffraction (XRD), Raman spectroscopy, X-ray photoelectron spectroscopy (XPS), Fourier-transform infrared spectroscopy (FTIR), Brunauer-emmett-teller (BET), thermogravimetric analysis (TGA) and electrical conductivity. Meanwhile the dispersion stability and physical properties of the graphene-based inks via visual observation, zeta potential analysis, UV-Vis spectrophotometer, HRTEM, viscosity and wettability were investigated.

1.5 Thesis overview

This thesis consists of five chapters. Chapter 1 (Introduction) discusses the introduction of the overall research by introducing graphene, conductive ink and printing methods for graphene-based inks and printing pattern productions. The

motivations for conducting present study are expressed after identifying current hurdles related to the highly toxic (hazardous) and high boiling point solvent in the production of graphene ink. Based on that, a set of objectives are then outlined. This chapter ends with the description about the scope of study and thesis overview by chapters.

Chapter 2 (Literature Review) gives an overview of the recent progress in conductive inks which include graphene ink, other conductive materials ink and graphene-conductive material hybrid ink, respectively. Besides that, the properties of the conductive inks are also discussed. The printing techniques for the fabrication of flexible electronics and the overview of research work are summarized.

Chapter 3 (Materials and Method) describes the materials and methods used throughout this study. Detailed information on the materials, chemicals, equipment and methodologies to conduct the experimental works are described within this chapter. The characterization techniques are also discussed in this chapter.

Chapter 4 (Results and Discussion) is the heart of this thesis where results and discussion are presented. It is divided into four sections. First section discusses the characterization of the synthesized GF and compare with commercial GNPs and SG. Second section covers the properties of graphene-based inks mixed with PV and conductive ink patterns fabricated using spray coating. Third section explores the stability of graphene-based materials dispersed into various types of alternative common solvents and mixed solvents. Finally, fourth section describes the production of conductive ink patterns using inkjet printing method.

Chapter 5 (Conclusion and Future Recommendations) presents the conclusions from this research and some recommendations for future studies in this related field.

CHAPTER 2

LITERATURE REVIEW

2.1 Conductive ink materials

Conductive ink becomes an important element in printing industry such as screen printing, spray coating, inkjet printing, gravure printing, *etc.* A conductive ink is a thermoplastic viscous paste that conducts electricity by inculcating conductive materials (Banfield, 2013). To be specific, the conductive inks are suspensions of conductive nanomaterials either in water or a solvent medium with or without an addition of a surfactant or polymer that acts as a stabiliser. These solvents must evaporate rapidly after deposition but not dry out quickly at the printhead nozzles while idle for short periods of time. To obtain high electrical conductivity of conductive inks, conductive nanomaterials are normally introduced; the sizes of these materials should be at least 50 times less than the printing nozzle to avoid clogging of the nozzles (Huang and Wu, 2019).

An ideal conductive ink should be inexpensive, simple to prepare, and offer good printability, low viscosity, good stability, good adhesion to the substrate, high electrical conductivity after printing and post-printing processing, and dry in preferentially densify manner at substrate surface without a coffee ring effect (Choi *et al.*, 2015; Liu *et al.*, 2015; Stoppa and Chiolerio, 2014). Coffee ring was formed on the printing substrate when a drop dries at room temperature, as obvious outflow induces edge growth process and forms ring-like pattern, as illustrated in Figure 2.1 (a). However, as the substrate temperature increases, the transition from a coffee ring to a uniform dried deposit was occurred, as presented in Figure 2.1 (b) (Li *et al.*, 2016; He and Derby, 2017).

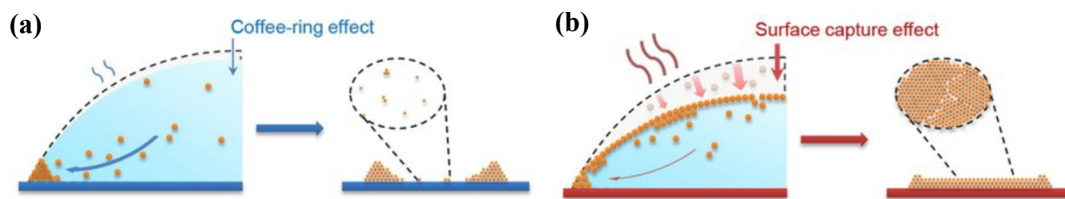


Figure 2.1 Schematic of (a) coffee-ring effect at low drying temperature and (b) surface capture effect at high drying temperature (Li *et al.*, 2016)

Various solvents have been widely studied to disperse graphene for conductive ink applications and interfacial tension can be considered as one of the main criteria on graphene dispersion. Higher interfacial tension between solid and liquid often leads to poor stability of the dispersion (Israelachvili, 2011). Coleman (2012) reported that solvents with the surface tension of approximately 40 mNm^{-1} can minimize their interfacial tension with graphene. Hernandez *et al.* (2008) and Khan *et al.* (2011) reported that NMP is considered to be the most widely used solvent for dispersing graphene and the sonication of graphite with N-Methyl-2-pyrrolidone (NMP) can produce stable graphene dispersion at concentration between 0.01 to 2 mgmL^{-1} . Majee *et al.* (2016) produced stable graphene ink at high concentration of 3.2 mgmL^{-1} using shear exfoliation of graphite in NMP. Other solvents including Dimethyl sulfoxide (DMSO) and N,N-Dimethylformamide (DMF) have also been established as effective solvents to prepare graphene ink with good dispersion stability (Li *et al.*, 2013; Tran *et al.*, 2018). However, these solvents suffer from high boiling point ($>150^\circ\text{C}$) which restricted them to be used with plastic substrates, as it requires low treatment temperature. Besides that, these solvents are expensive and highly toxic making them not practical to be widely utilized in the industry.

Due to that, low boiling point and less toxic solvents are preferable. Several examples of common low boiling point solvents including acetone and ethanol were alternatively used, however, these solvents have low surface tension ($<30 \text{ mJm}^{-2}$) that lead to poor graphene dispersion. Table 2.1 describes the chemical properties such as surface tension, boiling point and chemical formula of common solvents used for graphene ink dispersion.

Table 2.1 Chemical properties of common solvents used for graphene ink dispersion
(Materials Safety Data Sheet; DataPhysics Instruments GmbH)

| Solvent | Chemical formula | Surface tension (mNm^{-1}) | Boiling point ($^{\circ}\text{C}$) |
|-----------------------|-----------------------------------|--|---|
| NMP | $\text{C}_5\text{H}_9\text{NO}$ | 40.8 | 202 |
| DMF | $\text{C}_3\text{H}_7\text{NO}$ | 37.1 | 153 |
| DMSO | $\text{C}_2\text{H}_6\text{OS}$ | 43.5 | 189 |
| 2-propanol (IPA) | $\text{C}_3\text{H}_8\text{O}$ | 23 | 83 |
| Tetrahydrofuran (THF) | $\text{C}_4\text{H}_8\text{O}$ | 26.4 | 66 |
| 1,2-Dichlorobenzene | $\text{C}_6\text{H}_4\text{Cl}_2$ | 36.6 | 181 |
| Cyclohexanol | $\text{C}_6\text{H}_{12}\text{O}$ | 34.4 | 162 |
| Chlorobenzene | $\text{C}_6\text{H}_5\text{Cl}$ | 33.6 | 131 |
| Toluene | C_7H_8 | 28.4 | 111 |
| Acetone | $\text{C}_3\text{H}_6\text{O}$ | 27.6 | 56 |
| Ethanol | $\text{C}_2\text{H}_6\text{O}$ | 22.1 | 78 |
| Water | H_2O | 72.8 | 100 |

2.1.1 Graphene-based ink

Since its isolation by Novoselov and Geim in 2004, graphene has attracted various investigations into its unique physicochemical, mechanical and electrical properties. Graphene has been considered as “the thinnest, most flexible and strongest material known” that conducts heat and electricity very well (Jaworski *et al.*, 2013; Brownson and Banks, 2014). Graphene has unique physicochemical properties with large specific surface area ($2630 \text{ m}^2\text{g}^{-1}$), high optical transparency (97.7%), extraordinary electron mobility ($200\,000 \text{ cm}^2\text{V}^{-1}\text{s}^{-1}$) and thermal conductivity ($5000 \text{ Wm}^{-1}\text{K}^{-1}$), extremely high mechanical strength (elastic modulus 0.25 TPa and tensile strength 42 Nm^{-1}) and possibility of mass-production at low cost (Shen *et al.*, 2012; Guo and Mei, 2014; Ghany *et al.*, 2017). These properties arise from the two-dimensional crystallographic nature of graphene. Table 2.2 describes the definitions of ‘graphene-like materials’ as proposed by Bianco *et al.* (2013).

Table 2.2 Comparison of graphene-like materials terms (Bianco *et al.*, 2013)

| Graphene terms | Details |
|----------------------------|--|
| Graphene layer | <ul style="list-style-type: none">• A single-atom-thick sheet of hexagonally arranged• sp^2-bonded carbon atoms and known as monolayer graphene |
| Turbostratic carbon | <ul style="list-style-type: none">• 3D sp^2-bonded carbon atoms and known as rotationally faulted• No defined registry of the layers• Prepared at low temperature and resist the development of 3D crystalline order upon very high temperature heat treatment |

Table 2.2 *Continued*

| | |
|--|---|
| Bilayer graphene, trilayer graphene | <ul style="list-style-type: none">• 2D (sheet-like) materials• Consists 2 or 3 well-defined, countable and stacked graphene layers of extended lateral dimension |
| Multi-layer graphene | <ul style="list-style-type: none">• 2D (sheet-like) material• Consists of a small number (between 2 to 10) of well defined, countable and stacked graphene layers of extended lateral dimension |
| Few-layer graphene | <ul style="list-style-type: none">• 2D (sheet-like) material• A subset of multi-layer graphene with layer numbers from 2 to 5 |
| Graphite nanoplates, graphite nanosheets, graphite nanoflakes | <ul style="list-style-type: none">• 2D graphite materials• Thickness and/or lateral dimension less than 100 nm |
| Graphene microsheet | <ul style="list-style-type: none">• A single-atom-thick sheet of hexagonal arranged sp^2-bonded carbon atoms that is not an integral part of a carbon material but is freely suspended• Lateral dimension between 100 nm to 100 μm |
| Graphene oxide (GO) | <ul style="list-style-type: none">• Chemically modified graphene prepared by oxidation and exfoliation, followed by extensive oxidative modification of the basal plane• Monolayer material with a high oxygen content |
| Reduced graphene oxide (rGO) | <ul style="list-style-type: none">• GO that has been reductively processed by chemical, thermal, <i>etc</i> methods to reduce its oxygen content |

To date, several methods for the production of graphene have been explored, and these methods are divided into two categories: (1) bottom-up approach (from carbon precursors) i.e. elaboration on silicon carbide, chemical vapour deposition, solvothermal reaction, *etc*, and (2) top-down approach (from graphite) i.e. micromechanical cleavage, liquid phase exfoliation, chemical reduction of GO and exfoliation of graphite intercalation compounds, *etc*. The various graphene elaboration methods allow a wide choice in terms of size, quality and price depending on the applications. Figure 2.2 depicts the comparison of quality against price (for mass production) for graphene elaboration methods. Most graphene that were used in electronic applications are fully dependent on the quality of the prepared graphene, types of defects, substrate, *etc* which strongly affected by the production method (Novoselov *et al.*, 2012). The bottom-up approaches can produce graphene with fewer defects; however, these methods suffer from high complexity, low yield and the high cost of metal substrates. Meanwhile, top-down approaches produce graphene in high yield, use solution-based processability and are easy to implement due to the use of the existing form of a bulk material (Chen *et al.*, 2004; Choucair *et al.*, 2009; Novoselov *et al.*, 2012; Low *et al.*, 2013, Speyer *et al.*, 2015).

Graphene foam (GF) also known as 3D graphene, is one of the graphene-like materials and can be synthesized using various bottom-up approaches including solvothermal method. As reported by Jiang and Fan (2014) and Liu *et al.* (2014), GF has a unique porous structure, unlike sheet-like structure as seen in 2D graphene-like materials. GF also has a very large specific surface area compared to other common graphene-like materials due to the 3D topography which prevents the restacking generally observed in 2D graphene-like materials. The voids with micron-scale were separated by thin carbon walls, as illustrated in Figure 2.3.

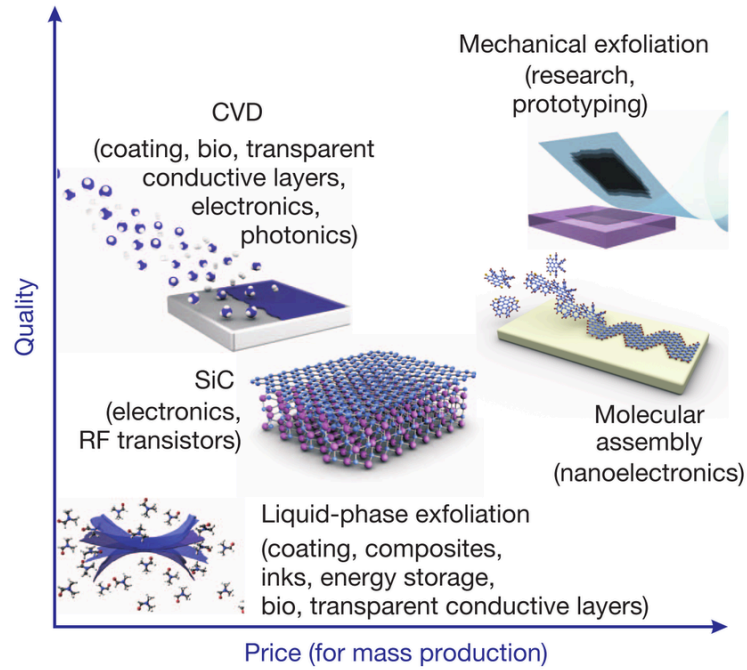


Figure 2.2 Comparison of quality against price (for mass production) for graphene elaboration methods (Novoselov *et al.*, 2012)

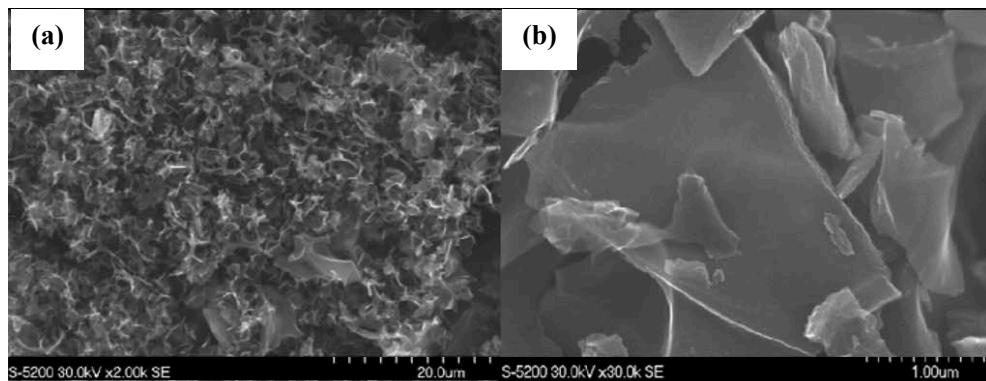


Figure 2.3 SEM images of graphene foam (GF) (Liu *et al.*, 2014)

Graphene conductive inks have the potential to revolutionize the printed conductor field by replacing metallic inks, conductive polymer inks and other carbon material inks, while at the same time reducing biological hazards and production costs (Arapov *et al.*, 2014). Huang *et al.* (2011) reported that a series of inkjet printing processes using water-soluble single-layered GO (SGO) and few-layered GO (FGO)

have been printed on diverse flexible substrates. Based on these findings, the electrical conductivity of GO and FGO after 25 printed layers on a polyimide (PI) substrate are $5.0 \times 10^2 \text{ Sm}^{-1}$ and $9.0 \times 10^2 \text{ Sm}^{-1}$, respectively. According to Huang *et al.* (2011), the low conductivity of GO printed on PI substrate compared to FGO could be attributed to the high number of oxygen-containing groups in the GO sample (Figure 2.4).

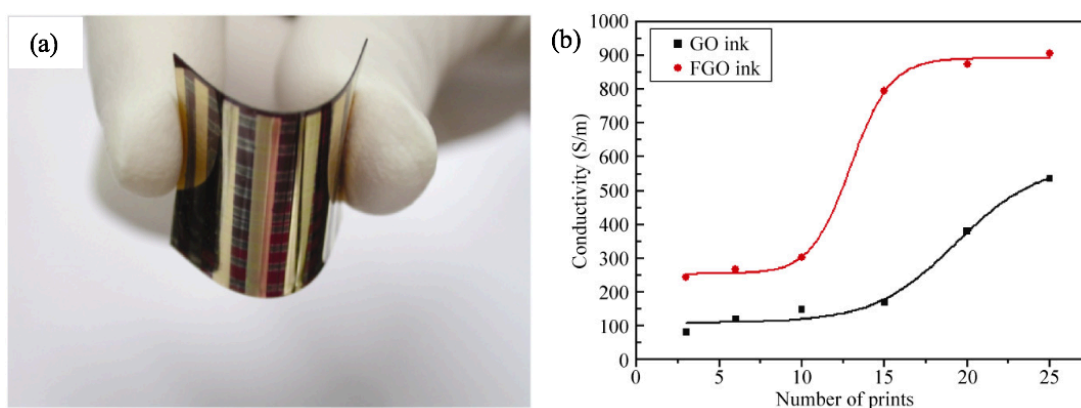


Figure 2.4 (a) Photograph of a printed pattern on PI substrate and (b) the electrical conductivity of the printed patterns on PI (Huang *et al.*, 2011)

Arapov *et al.* (2014) presented a comparison of two graphene inks: one prepared by the solubilisation of expanded graphite in the presence of a surface-active polymer and the other by covalent graphene functionalisation followed by redispersion in a solvent but without surfactant. Based on their findings, the conductivity levels for expanded graphite-based inks and functionalised graphene are approximately $1\text{--}2 \text{ k}\Omega\text{sq}^{-1}$ and $2 \text{ M}\Omega\text{sq}^{-1}$, respectively, for 15 printed layers. This technique is simple and efficient, and therefore has a potential to be used for large-area printing of conductive films. Meanwhile, Gao *et al.* (2014) fabricated highly conductive pristine graphene electrodes by inkjet printing using ethyl cellulose-stabilised ink prepared from pristine graphene. No graphene sheets were observed to settle at the bottom of the bottle even

after 9 months. This stability is reported to be due to the strong hydrophobic interactions between ethyl cellulose (as the stabilising polymer) and the graphene sheets countering the van der Waals forces between the graphene flakes, thereby inhibiting the aggregation of the graphene. The printed films have high conductivity with the value of $9.24 \times 10^3 \text{ Sm}^{-1}$ after 30 printed layers annealed at 300 °C for 30 min.

In 2016, Miao *et al.* reported a simple method of inkjet printing of graphene nanoplatelets (GNPs) using an electrochemical process in an inorganic-salt-based electrolyte without using stabiliser. The electrical conductivity of printed pristine GNPs film improved from 44 Sm^{-1} to approximately $2.5 \times 10^3 \text{ Sm}^{-1}$ after 20 printed layers after a simple thermal treatment of annealing at 300 °C for 1 h (Figure 2.5). Meanwhile, Majee *et al.* (2017) reported an efficient inkjet printing of water-based pristine GNPs ink by a shear-exfoliation process with the aid of bromine intercalation in aqueous media using a water-soluble cellulose stabiliser, i.e. (hydroxypropyl)methyl cellulose. The electrical conductivity was $1.4 \times 10^3 \text{ Sm}^{-1}$ when the printed GNPs film was dried at 100 °C and increased to about $3 \times 10^4 \text{ Sm}^{-1}$ after an additional treatment of dipping the film in an aqueous iodine solution prior to drying. In contrast, a conductivity of about $2.4 \times 10^4 \text{ Sm}^{-1}$ was obtained after annealing the film at elevated temperature in air. The electrical conductivity of the doped GNPs films improved further to 10^5 Sm^{-1} after annealing in air at 300 °C. This shows a positive effect of the combination of iodine doping and thermal annealing on conductivity enhancement for printed GNPs films. In 2017, Secor *et al.* demonstrated graphene inks with nitrocellulose as a synergistic polymer stabiliser. The printed graphene films on glass had electrical conductivity values of $1.0 \times 10^4 \text{ Sm}^{-1}$ and $4.1 \times 10^4 \text{ Sm}^{-1}$ when annealed at 200 °C and 350 °C, respectively.

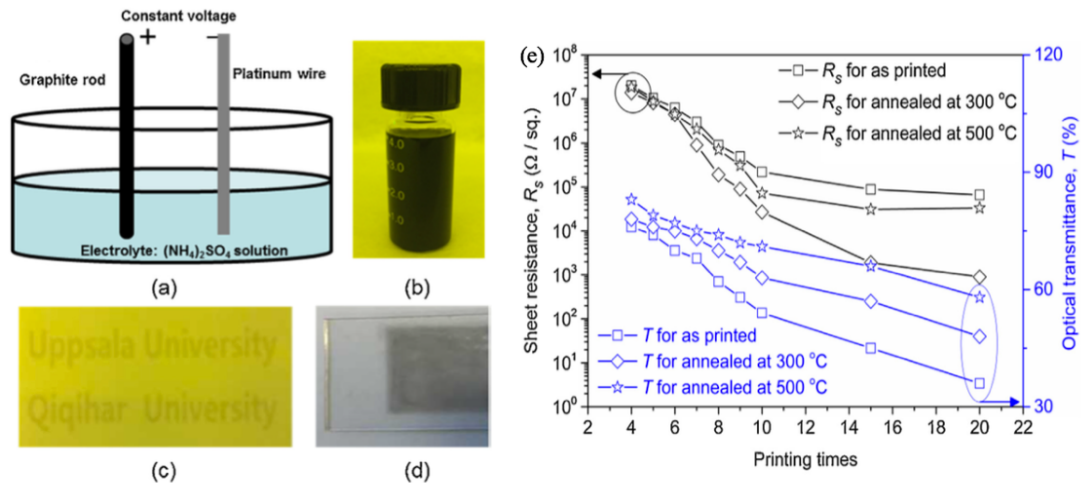


Figure 2.5 (a) Schematic experimental setup for the electrochemical exfoliation process, photo pictures of (b) electrochemical-GNPs ink ready for inkjet printing, (c) printed patterns on a plastic substrate and (d) printed test sample on a glass substrate, and (e) variations of sheet resistance and optical transmittance with number of prints at different annealing temperatures (Miao *et al.*, 2016)

Table 2.3 presents the comparison of graphene-based inks and electrical properties based on the literature. It is observed that graphene inks based on various types of graphene-like materials have been successfully synthesized using sonication as mixing method and inkjet printing as a fabrication method. Based on Table 2.3, most of the graphene-based inks were prepared using GNPs, GO and rGO as the fillers. From the findings, it can be observed that types of solvent, number of printed layers, annealing temperature and type of substrate influenced the electrical properties of the printed films. However, higher annealing temperature (100 – 350 °C) and longer annealing duration (> 30 min) of printed graphene films restricted the used of polymer substrate for the fabrication of flexible printed electronics.

Table 2.3 Comparison of the various types of graphene inks and electrical conductivity from literature (Huang *et al.*, 2011; Secor *et al.*, 2013; Gao *et al.*, 2014, Secor *et al.*, 2015; Miao *et al.*, 2016, Majee *et al.*, 2017; Secor *et al.*, 2017)

| Graphene material | Solvent and surfactant | Substrate | Printing layers | Electrical conductivity (Sm⁻¹) |
|------------------------------|---|---|------------------------|---|
| SGO and FGO | Deionized water | Polyimide (PI) and PET | 25 | 5.5 X 10 ² (SGO) and 9.0 X 10 ² (FGO) |
| Graphene and ethyl cellulose | Cyclohexanone and terpineol | Si/SiO ₂ wafers | 10 | 2.5 X 10 ⁴ |
| Pristine graphene flakes | Ethyl cellulose and cyclohexanone | Hexamethyldisilazane-treated glass slides | 30 | 9.24 X 10 ³ |
| Graphene and ethyl cellulose | Cyclohexanone and terpineol | Poly(ethylene naphthalate) (PEN) | (not mentioned) | 2.5 X 10 ⁴ |
| Electrochemical GNP | DMF, EG and glycerol | Plastic and glass | 20 | 2.5 x 10 ³ |
| GNPs | Water soluble cellulose | Glass and PET | 20 | 10 ⁵ |
| Graphene and nitrocellulose | Ethyl lactate, octyl acetate, ethylene glycol diacetate | Glass | (not mentioned) | 1.0 X 10 ⁴ (200 °C) and 4.1 X 10 ⁴ (350 °C) |

2.1.2 Other conductive materials-based ink

2.1.2(a) Ink based on conductive nanomaterials

Other than graphene, several types of commonly used conductive materials are also reported in the literature. Silver nanoparticles (AgNPs) are another promising nanomaterial for flexible electronics. Until now, AgNPs-based inks have represented the most important commercial nanotechnology-derived product and the one most widely studied worldwide, other than graphene (Rajan *et al.*, 2016). Kastner *et al.* (2017) investigated and optimised the printing of a reactive silver ink made of silver acetate dissolved in aqueous ammonium hydroxide. Based on the findings, the conductivity value of the printed film on glass was $4.42 \times 10^6 \text{ Sm}^{-1}$ after annealing at $120 \text{ }^\circ\text{C}$ for several minutes, with the pattern thickness ranging from 150 to 133 nm. For printed silver films on acrylate-based coatings, the conductivity value was $2.9 \times 10^5 \text{ Sm}^{-1}$ with a pattern thickness of 150 nm.

Besides that, gold nanoparticles (AuNPs) are known as the most stable metal nanoparticles and have been used in printing highly conductive elements. The unique properties of AuNPs make them useful in various applications, such as colourants, metal coatings, electronics, optics and chemical catalysis (Iwakoshi *et al.*, 2005). Despite the excellent electrical conductivity and excellent printability of AgNPs and AuNPs, various work still needs to be done considering the high cost and high sintering temperature ($>200 \text{ }^\circ\text{C}$) and long sintering required, which make them inadvisable for use on a large scale, especially in industrial applications and not compatible for flexible polymer substrates such as PEN and PET due to their low glass-transition temperatures (Kamyshny *et al.*, 2005; Kim *et al.*, 2014).

Copper nanoparticles (CuNPs) are a good alternative for gold and silver nanoparticles due to their high electrical conductivity and low price (Tsai *et al.*, 2015). However, the main problem of CuNPs is that they are easily oxidised under heat and humidity conditions, which limits their applications. It is also difficult to produce homogeneous nanoparticles and ensure good dispersion within the ink, as the material is not stable in most common solvents (i.e. water, isopropyl alcohol, acetone, *etc*) which causes sedimentation (Lee *et al.*, 2008).

Carbon nanotubes (CNTs) have drawn considerable attention over other nanomaterials by being electrically heterogeneous (either metallic or semiconducting) in nature. This makes them attractive for numerous applications in electronics (Denneulin *et al.*, 2011). However, the stability of CNTs suspensions in water is still a topic of interest because the nanoparticles tend to aggregate easily due to their high van der Waals forces of attraction; moreover, there are toxicological issues. Besides that, CNTs require selective growth, functionalisation and sorting processes for separation in order to exploit in full their electronic properties (Sabba and Thomas, 2004; Kernan and Blau, 2008).

2.1.2(b) Ink based on conductive polymers

Several conductive polymers have been intensively investigated, considering their low cost and that no sintering process is required; in particular, polyaniline (PANI), polypyrrole (PPy), poly(3,4-ethylenedioxythiophene)-poly(styrenesulfonate) (PEDOT:PSS), *etc*. PANI has been considered as one of the most promising conducting polymers due to its unique properties, including high electrical conductivity for a polymer material, excellent environmental stability and partial solubility in various solvents. It is the most versatile polymer due to its simplicity, low cost of preparation,

thermal and chemical stability and processability (Kulkarni *et al.*, 2013; Song *et al.*, 2015; Stempien *et al.*, 2015).

PPy is also a conducting polymer of moderate environmental stability and suitable for multifunctional applications. The electrical and physical properties of the polymeric films are fully dependant on the preparation conditions, such as the electrochemical method of polymerisation, concentration of monomer and doping agent and other synthesis conditions. The polymer is not conducting in its neutral state and only becomes conducting when it is oxidised. The conductivity value is in the range of 10^{-3} to $10^2 \Omega\text{cm}^{-1}$ (Schlenoff and Xu, 1992; Abdulla and Abbo, 2012; Popli and Patel, 2015).

PEDOT:PSS is a polymer mixture of poly(3,4-ethylenedioxythiophene (PEDOT) and polystyrene sulfonate (PSS). PEDOT:PSS is also regarded as one of the most technologically promising electrically conductive polymers, due to its water dispersibility, good electrical conductivity and excellent processability (Hong and Kanicki, 2004; Ha *et al.*, 2015; Sharbati, 2016). The electrical conductivity of pristine PEDOT:PSS dispersion is less than 10 Scm^{-1} and can be improved by post-treatment with some compounds such as ethylene glycol (Groenendaal *et al.*, 2000; Kim *et al.*, 2011; Abroshan *et al.*, 2011).

Table 2.4 represents the brief comparison between existing inks made of several types of conductive polymers with conductive nanomaterials.

Table 2.4 Comparison of several types of conductive materials-based inks (Kordás *et al.*, 2006; Lee *et al.*, 2008; Kang *et al.*, 2010; Cui *et al.*, 2010; Nie *et al.*, 2012; Perinka *et al.*, 2013; Zhang *et al.*, 2015; Kastner *et al.*, 2017)

| Ink material | Sintering temperature (°C) | Resistivity (Ωcm)/ Surface resistance (Ωsq^{-1})/ Conductivity (Scm^{-1}) |
|----------------|----------------------------|--|
| AuNPs | (not mentioned) | $0.8 \times 10^5 \text{ Scm}^{-1}$ |
| AgNPs | 150 | $17 \mu\Omega\text{cm}$ |
| | 230 | $3.1 \mu\Omega\text{cm}$ |
| AgNPs | 30 | $31.6\text{-}26.5 \mu\Omega\text{cm}$ |
| AgNPs | 120 | $4.42 \times 10^6 \text{ Scm}^{-1}$ |
| CuNPs | 200 | $3.6 \mu\Omega\text{cm}$ |
| CuNPs | 200 | $36.7 \text{ n}\Omega\text{m}$ |
| PEDOT:PSS | (not mentioned) | 1.1 mScm^{-1} |
| MWCNT | (not mentioned) | $40 \text{ k}\Omega\text{sq}^{-1}$ |
| MWCNT-COOH | (not mentioned) | $1.1 \times 10^6 \Omega\text{sq}^{-1}$ |
| MWCNT-COOH-PSS | (not mentioned) | $3.5 \times 10^3 \Omega\text{sq}^{-1}$ |

2.1.3 Graphene hybrid-based ink

Recently, researches on graphene hybrid inks by adding metallic nanoparticles or conductive polymers to improve the original properties of graphene have been widely developed. Based on the comparison of literature review on graphene hybrid-based inks